



Temperature sensor integrated curl resonator chipless RFID tag for high capacity data identification applications

Hend A. Malhat¹ · Esraa A. El-Refaay² · Saber H. Zainud-Deen¹

Received: 29 September 2021 / Accepted: 29 October 2022 / Published online: 13 November 2022
© The Author(s) 2022

Abstract

This paper proposes a compact multi-bits chipless RFID tag using fully printed resonators with dual performance of tagging and sensing temperature. Each bit is modelled as curl resonator coupled to microstrip line and is printed on metal-backed Rogers RO4003 substrate. The proposed model is characterized by high attenuation of -10 dB with narrow bandwidth and power reflection of -3.2 dB. A parametric study on the effect of the tag dimensions of the transmission coefficient response is introduced. The resonance frequency of each bit is controlled via controlling the curl arm's length. The multi-bits RFID tag is modelled using multi-curl resonators arranged next to microstrip line with different arm lengths. A multi-bits chipless RFID tags with 3-bits, 6-bits and 12-bits are designed in the frequency band from 3 to 7 GHz. The dimensions of 6-bits code are 60×17 mm² and for 12-bits code are 29.75×34 mm². A temperature sensing capability is achieved via integrated Stanyl polyamide material with the curl resonator. The first bit is used for temperature sensing while the other bits are used for data encoding. The proposed chipless RFID tags are simulated using commercial software based on well defined numerical techniques; i.e. high-frequency structure simulator (HFSS) based on finite element method (FEM) and verified with CST-microwave studio (CST-MWS) based on the finite integral technique (FIT).

1 Introduction

Radio frequency identification (RFID) is a wireless communication system, which use the radio waves in automatic identification of targets (Finkenzeller 2003). RFID technology is characterized by low fabrication cost, efficient performance, secure data transmission, and reliable solution to optical bar-code systems (Das 2006). The basic RFID system consists of reader, tag, and data processing system. The reader sends the signals to tag that contain the identification data of the object. The tag retransmit the signals loaded with the identification data back to the reader. Finally, the processing system is used to encode/decode the identification data from the reader and link it to

the mainframe for additional signal processing (Vena et al. 2012; Zainud-Deen et al. 2012, 2011a, b). Wide area of applications employs the RFID systems, as sports, medicine, supply chain, logistics, tracking, and luggage handling (Hirvonen 2008). The identification data is stored and processed in an IC-microchip embedded with the tag antenna. The existence of microchip limits the tag lifetime, cost and maintenance compared with conventional bar-codes (Preradovic and Karmakar 2010; Malhat et al. 2011; Zainud-Deen et al. 2009). Recently printed chipless RFID tags based on spectral signature data encoding have introduced to overcome the chip-based RFID systems drawbacks. The chipless RFID system operation is based on using two cross-polarized ultra-wideband (UWB) antennas in the tag and similarly in the reader (Ahson et al. 2008; Zainud-Deen et al. 2013). The UWB antenna transmit wide spectrum signal which will be encode large data bits using the tag multi-resonators as a cascaded stop-band filters. These multi-resonators introduces attenuation in the magnitude and a jump in the phase of the transmission coefficient spectrum. These abrupt logic “0” transitions in both magnitude and phase are recognized as at the reader end, while their absence are recognized as logic “1” (Preradovic and Karmakar 2012). The encoded data is

✉ Hend A. Malhat
er_honida1@yahoo.com

Esraa A. El-Refaay
engesraa.ahmed91@yahoo.com

Saber H. Zainud-Deen
anssaber@yahoo.com

¹ Faculty of Electronic Engineering, Menoufia University, Minuya, Egypt

² National Liver Institute, Menoufia University, Minuya, Egypt

Fig. 1 The detailed construction of the proposed curl resonator

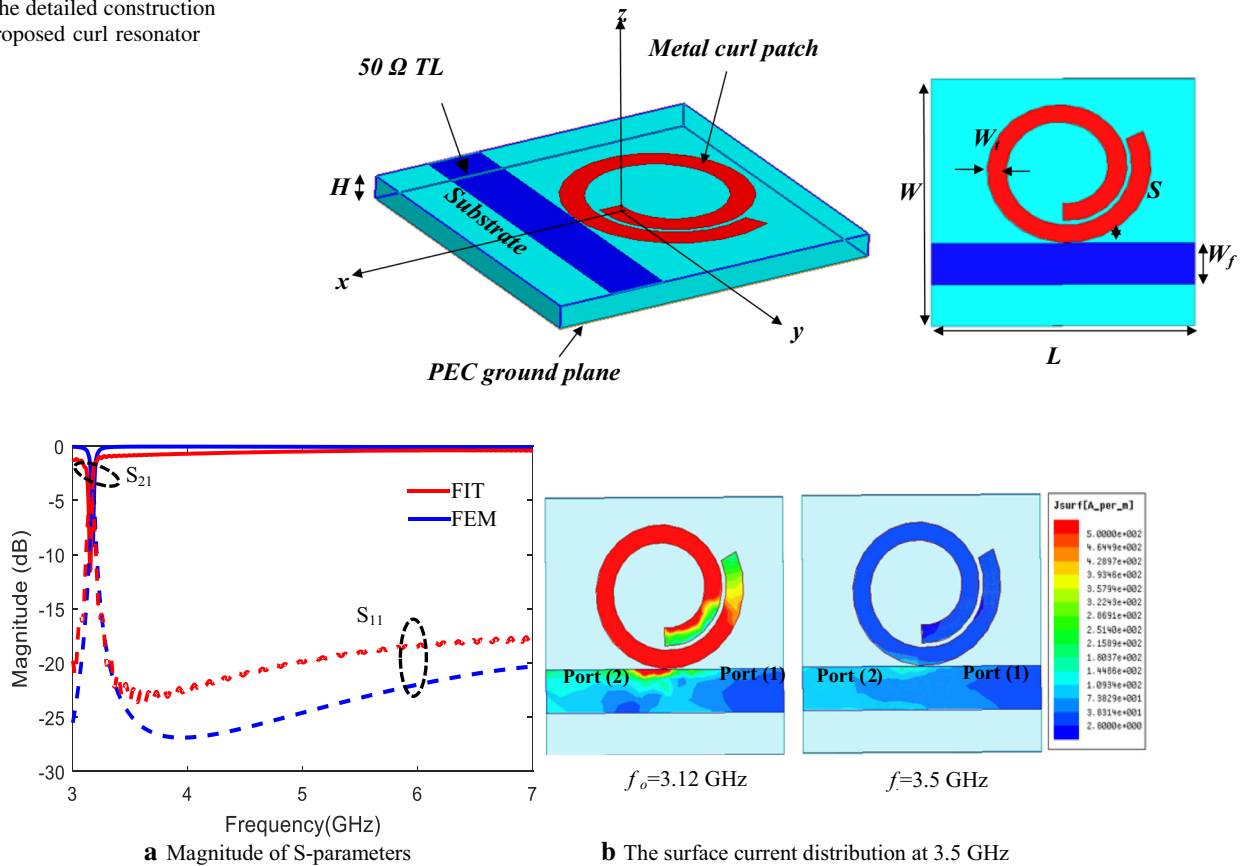


Fig. 2 The response of 1-bit chipless RFID tag calculated using CST-MWS and HFSS

retransmitted back to the reader through the cross-polarized UWB antenna. The radiation pattern of the UWB antenna is constant over the entire frequency band with omnidirectional distribution. Square UWB monopole antennas with simple and compact layout large bandwidth and figure of eight radiation pattern have been introduced in Yazdandoost and Kohno (2004) and Chen and Massey (2006).

Different techniques for chipless RFID tag design are introduced as space-filling curves and capacitive tuned dipoles are discussed in McVay et al. (2006) and Jalaly and Robertson (2005). The space-filling curves require further modifications to encode data. The capacitively tuned dipoles have large area and introduce undesired parasitic mutual coupling effects which degrades the data encoding efficiency. In (Preradovic et al. 2009), spiral resonator chipless tag operate at 2.37 GHz with 7 dB attenuation and -5.2 dB reflection. The dimensions of 6 bits spiral resonator code are 128.17×60 mm². A G-shape resonator chipless tag acts as a band stop filter is investigated in Abdulkawi et al. (2018). It operates at 3.85 GHz with 18 dB attenuation, and the dimensions of 10 bits G-shape resonator code are 60×30 mm². An equilateral triangle resonator coupled to microstrip line of 30×33.5 mm²

with -14 dB attenuation at 3.65 GHz has been introduced in Pawlikowski (2009). Smart functions are added to chipless RFID tags such as gas and temperature sensing. An optical transparent circular chipless tag with dual polarization and temperature sensing capability is investigated in Chung et al. (2005). In this paper, a compact chipless RFID tag based on curl resonator is designed for target identification from 3 to 7 GHz. The paper is organized as follows: Section 2 introduced the design of 1-bit and multi-bits curl chipless tag. Section 3 investigates the radiation characteristics of disk UWB monopole antenna. An integration of temperature sensor with the chipless curl tag is studied in Sect. 4. Finally, Sect. 5 concludes these results.

2 Design of chipless RFID tag

2.1 1-Bit chipless RFID Tag

A 1-bit compact chipless RFID tag configuration is shown in Fig. 1. The tag consists of curl-shaped resonator coupled to microstrip transmission line (TL) printed on a metal backed Rogers RO4003 substrate with $\epsilon_r = 3.55$, and \tan

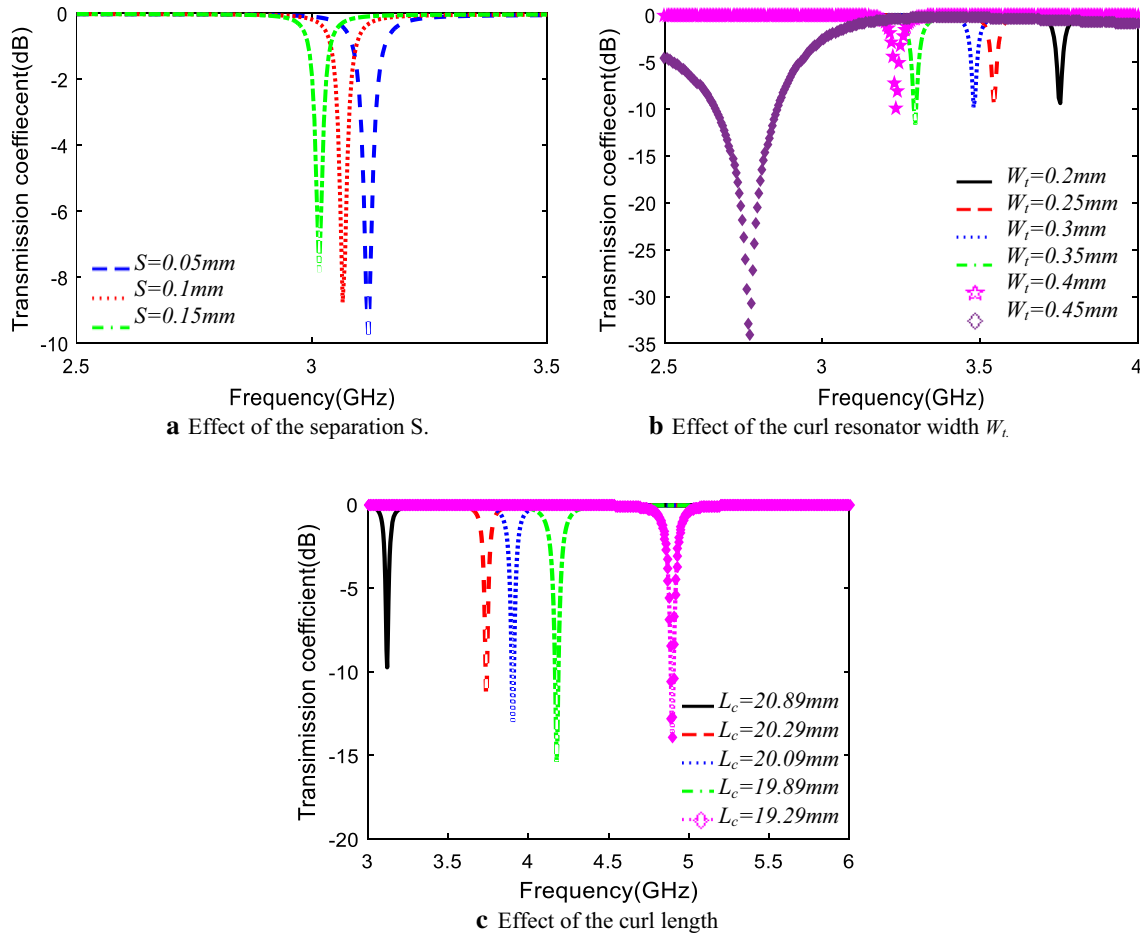


Fig. 3 The variation of the transmission coefficient versus frequency at different values design parameters

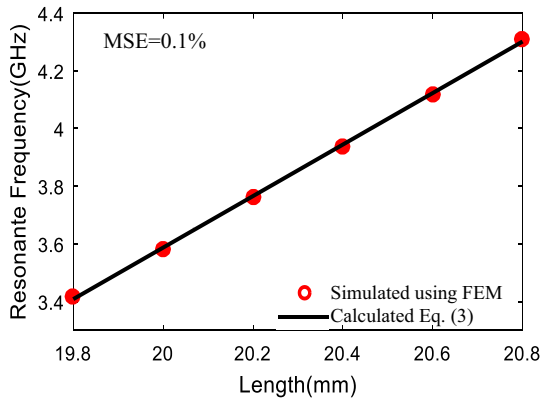


Fig. 4 The variation of resonance frequency versus curl arm length using MATLAB at $W_t = 0.4$ mm and $S = 0.05$ mm

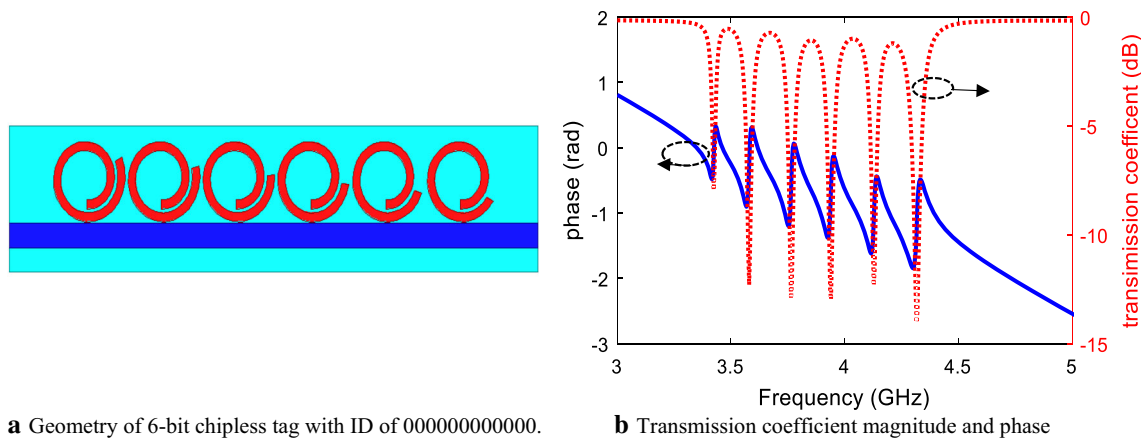
$\delta = 0.0027$. The 1-bit compact chipless RFID tag has total dimensions $L \times W \times H = 11 \times 17 \times 0.88$ mm³. The microstrip TL has width $W_f = 1.9$ mm to achieve an input impedance of 50 Ω . The locus point of the curl resonator (the analytical curve) follows the Archimedean function

and is given by http://cgtec.eu/wpcontent/uploads/Stanyl_brochure_02,

$$x = a\varphi' \cos \varphi' \tag{1}$$

$$y = a\varphi' \sin \varphi' \tag{2}$$

where $a = 0.1257$ is the curl constant and φ' is the winding angle starting at φ_{st} and ending at φ_{end} . The resonator is designed to operating at 3.12 GHz, with dimensions: $w_t = 0.4$ mm, $\varphi_{st} = 12.57$ rad and ending at $\varphi_{end} = 20.89$ rad. The S-parameters versus frequency for the 1-bit tag are shown in Fig. 2a. The structure acts as a band stop filter with good insertion loss. The CST-MWS and HFSS are used to analyze the 1-bit RFID tag by applying open and space boundary in all directions except in the $\pm y$ axis where open boundary applies. Two waveguide ports are placed along the TL ends with impedances set to 50 Ω . The S_{21} curve of the curl antenna resonator shows resonant at 3.12 GHz with 9.7 dB attenuation. The corresponding S_{11} curve has a magnitude of 3.27 dB, where total coupling occurs from port (1) to port (2). Good agreement between results calculated using CST-









a Geometry of 6-bit chipless tag with ID of 000000000000.

b Transmission coefficient magnitude and phase

Fig. 5 The frequency response of 6-bit chipless tag with ID of 000000 calculated using HFSS

Table 1 The curl length corresponding to resonator bits of code 000000

Shapes						
Code	0	0	0	0	0	0
L_c (mm)	20.89	20.69	20.49	20.29	20.09	19.89

MWS and that calculated using HFSS is noticed around the resonance frequency. The mismatch between calculated results at the higher frequencies is due to the different meshing mechanism in both simulation programs. Figure 2b shows a graphical plot for the surface current distribution using HFSS at the resonant frequency 3.12 GHz and a non-resonant frequency 3.5 GHz. The proposed sensor has a stop-band behavior at the CSRR resonant frequency. At the resonant frequency 3.12 GHz, the curl antenna resonator has a low impedance path to the ground and thus absorbs most of the current flowing through the TL from port (1) toward port (2). No current appears at port (2) and the stop-band response occurs. At the non-resonant frequency 3.5 GHz, the complementary split ring resonator (CSRR) couples the current to port (2).

A parametric study on the curl shape design parameters on the S_{21} response is presented. The separation between the curl resonator and the transmission line S is changed from 0.05 to 0.15 mm while keeping the other design parameters constant as shown in Fig. 3a. The resonance of the transmission coefficient is decreased with increasing the separation, S , and the magnitude of S_{21} is decreased. The optimum value of S is 0.05 mm. The variations of curl shape width W_t from 0.2 to 0.45 mm are shown in Fig. 3b. Increasing the curl shape width W_t shifts the resonant frequency to the lower side. The magnitude of the transmission coefficient of the curl shape width W_t is mainly

constant and unaffected by the parameters variations. However, for $W_t = 0.45$ mm, the S_{21} is increased but the bandwidth is increased. The optimal curl shape width W_t is 0.4 mm. By varying the length of the curl shape L_c , the resonant frequency is varied as shown in Fig. 3c. Each curl shape resonator introduces a different stop band resonance. Figure 4 shows the variation of the curl resonant frequency with the curl arm length L_c . As expected, the resonant frequency of the curl resonator increases as the length of the curl shape decreases and vice versa. This response is modelled using equation with mean square error (MSE) of 0.1% using MATLAB given by:

$$f_o = 0.89L_c - 14.27 \quad (3)$$

2.2 Multi-bits chipless RFID tag

In order to design the curls at different frequencies, the length of each curl has been varied so that the curl's resonant frequency is tuned. Each curl resonator has a different length which introduces a different stop band resonance. The presence of the resonance will stop a particular frequency resulting in the signal being attenuated at that frequency when retransmitted to the reader. This can be used to encode logic "0" based on magnitude levels. The absence of the resonance will be retransmitted with minimum attenuation due to the absence of the stop-band, this would represent logic "1". Each curl resonator has a different length which introduces a different stop band resonance. The 6-bit tag consists of six curl resonators separated by distance 0.3 mm and cascaded next to a 50 Ω microstrip line as shown in Fig. 5a. The multi-resonator provides six distinguishable resonances between 3.4 and 4.4 GHz. Each resonant frequency is separated by approximately 200 MHz from each other. The tag has a 6-bit ID where the most significant bit (MSB) corresponds to the highest resonant frequency at 4.5 GHz and the least

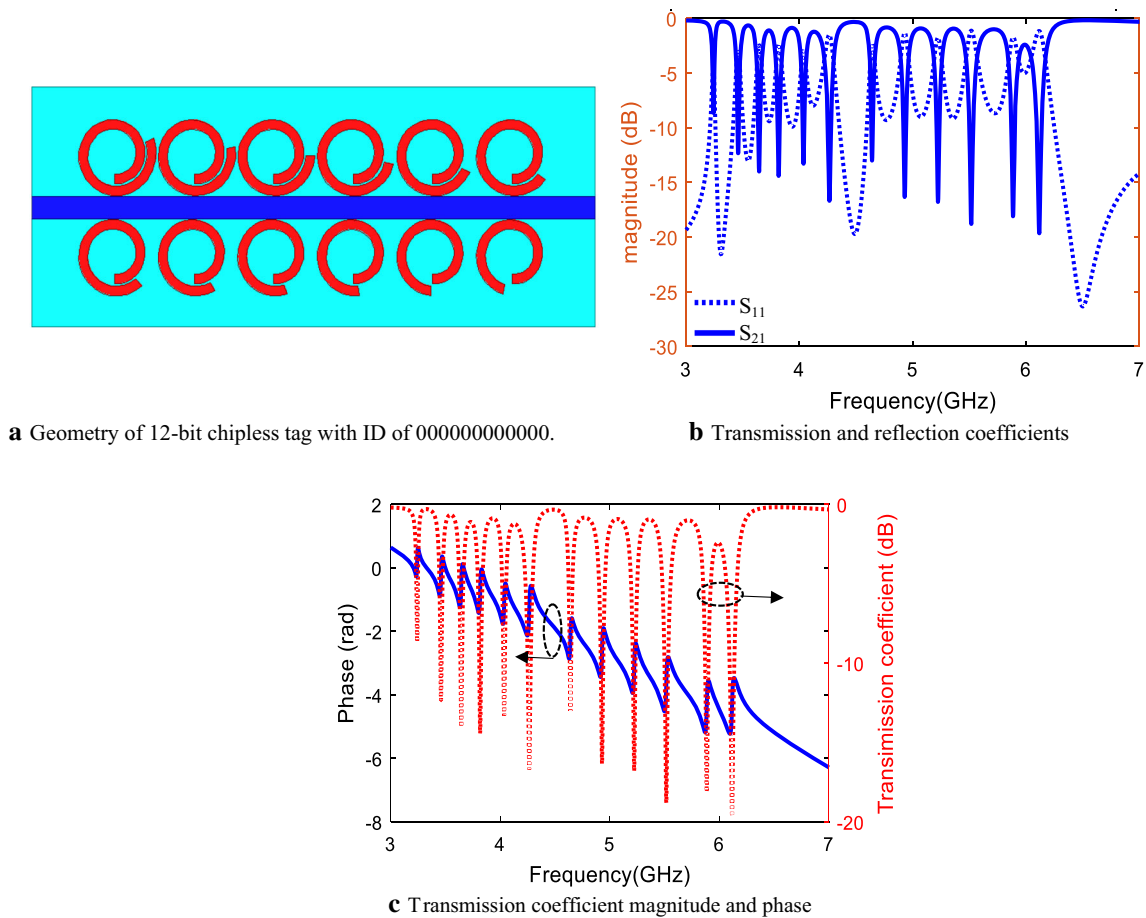


Fig. 6 The frequency response of 12-bit chipless tag with ID of 000000000000 calculated using HFSS

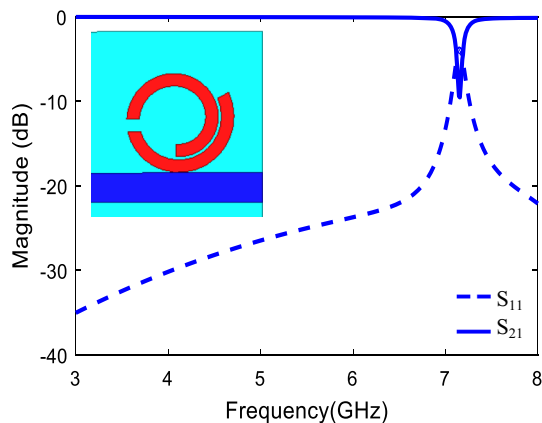


Fig. 7 The simulated transmission and reflection coefficients versus frequency for cut-circuited curl logic bit (1) calculated using HFSS

significant bit (LSB) corresponds to the lowest resonant frequency at 3.4 GHz. Figure 5b. shows the simulated frequency response in both magnitude and phase of the 6-bit tag. At the resonant frequencies magnitude “dip” and phase “jump” in the magnitude and phase of the transmission coefficient spectrum is observed. The curl length

(in mm) of each the 6 bits code is illustrated in Table 1. Additional 6-bits with different resonant frequencies are achieved by make mirror of six curl around the microstrip TL to produce 12-bits tag. The transmitter/receiver 12-bits are achieved approximately with the same distance as shown in Fig. 6. Figure 6 shows the simulated frequency response in both magnitude and phase of the 12-bit tag. The tag provides twelve distinguishable resonances frequencies between 3 to 7 GHz.

2.3 Changing logic state of the chipless tag

Encoding the data into the tag to have a unique ID is performed by introducing or removing the resonances of the multi-resonator. In order to simulate bit 1, it can be achieved by removing the curl, or by cut the curl as shown in Fig. 7. The resonant frequency of the curl is shifted-up to frequency where it will become of no significance. The advantage of cutting the curl instead of removing the entire curl from the layout is the fact that it enables future printing techniques to preserve the layout with all of the curl cut. Encoding data is achieved by cutting can be

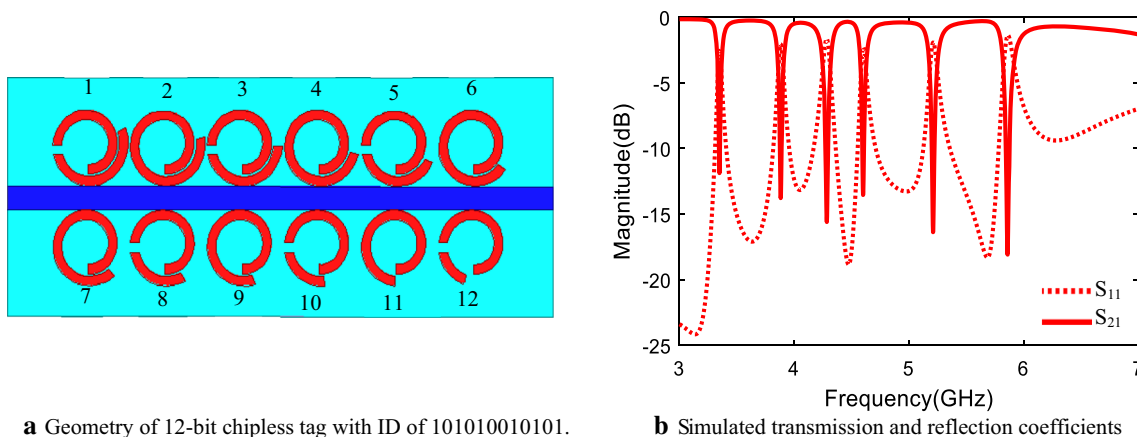


Fig. 8 The frequency response of 12-bit chipless tag with ID of 101010010101 calculated using HFSS

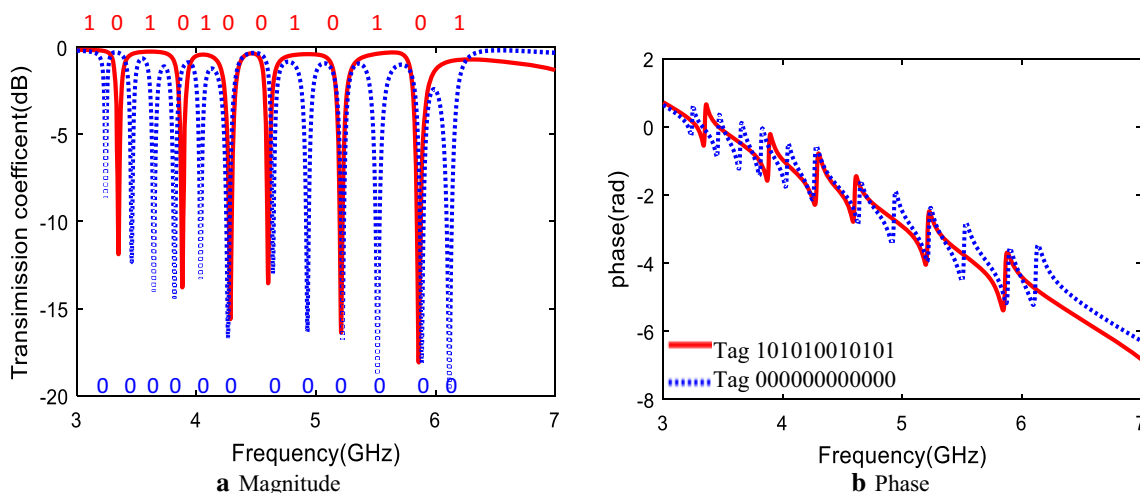


Fig. 9 The transmission coefficient of 12-bit chipless tag with ID of 101010010101 calculated using HFSS

Table 2 The curl length corresponding to resonator bits of code 101010010101

Shape												
Codes	1	0	1	0	1	0	0	1	0	1	0	1
Length (mm)	20.89	20.69	20.49	20.29	20.09	19.89	19.69	19.49	19.29	19.09	18.89	18.69

obtained via a laser or other etching technique. In order to create a different ID, for example 101010010101, the resonances at frequencies are removed via cutting their corresponding curls as shown in Figs. 8 and 9. The curl length of 12 bits’ code is illustrated in Table 2. The frequency signatures of tags with different ID’s and their corresponding curls with ID 000111111000 are shown in Fig. 10. Figure 11 shows the 12 bits chipless tag and the transmission coefficient for ID 001100110011. The

different codes are clearly represented in magnitude and phase information of the transmitted signal.

3 UWB disc-loaded monopole antennas for chipless RFID tag (3–18 GHz)

The UWB monopoles need to be fully planar and printable. The UWB monopole antenna is printed on a substrate that is made on a substrate Rogers RO4003 with dielectric

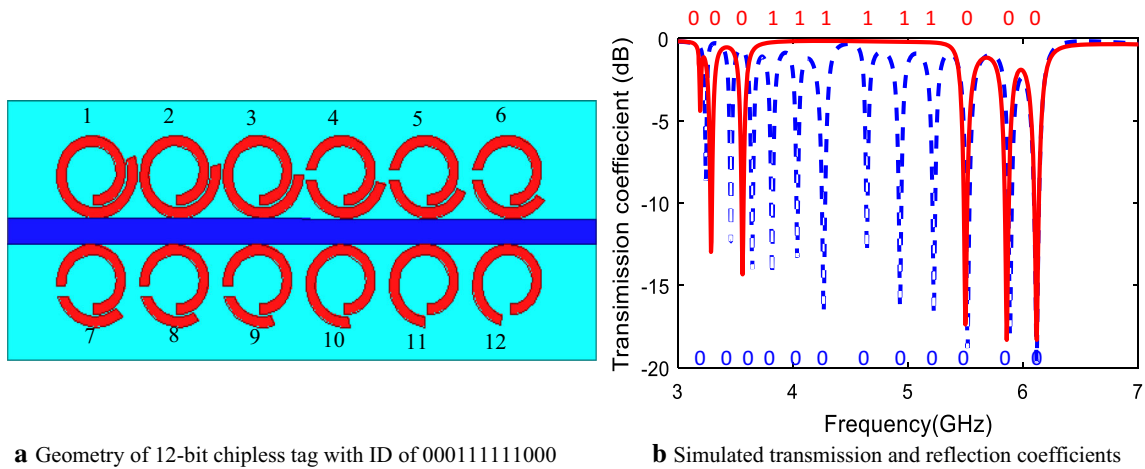


Fig. 10 The frequency response of 12-bit chipless tag with ID of 000111111000 calculated using HFSS

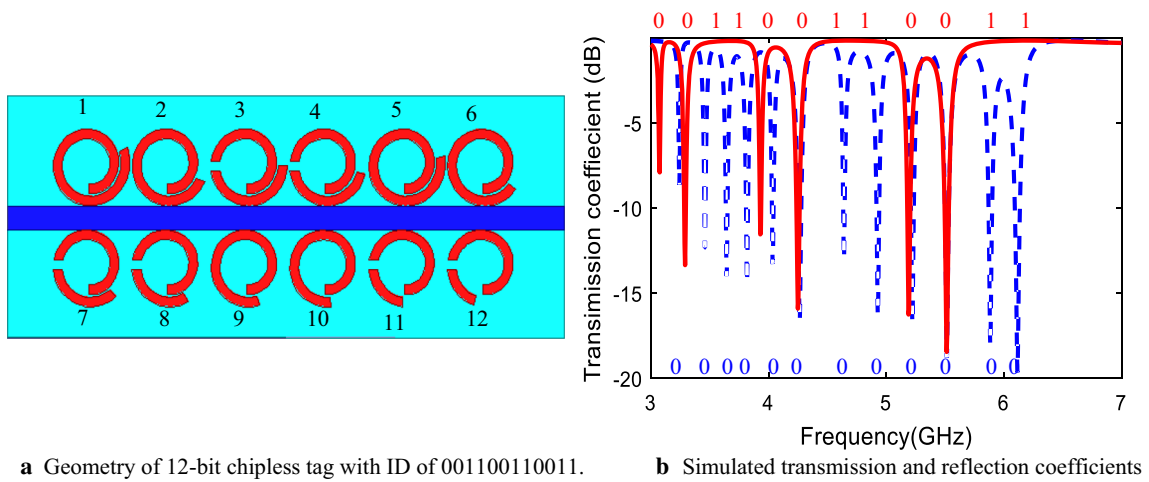


Fig. 11 The frequency response of 12-bit chipless tag with ID of 001100110011 calculated using HFSS

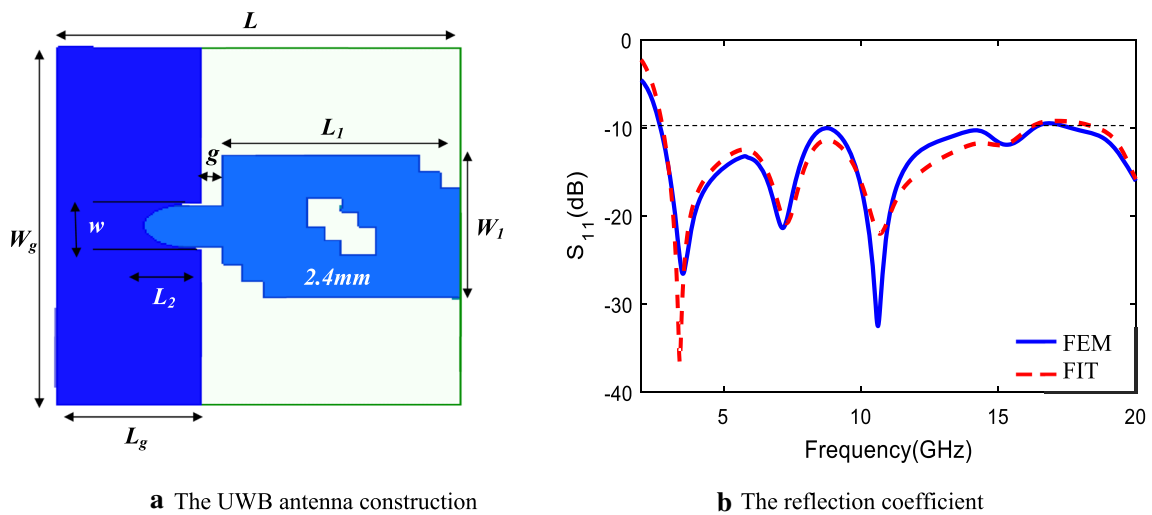


Fig. 12 The geometry of UWB monopole antenna and the frequency response of the reflection coefficient calculated using CST-MWS and HFSS

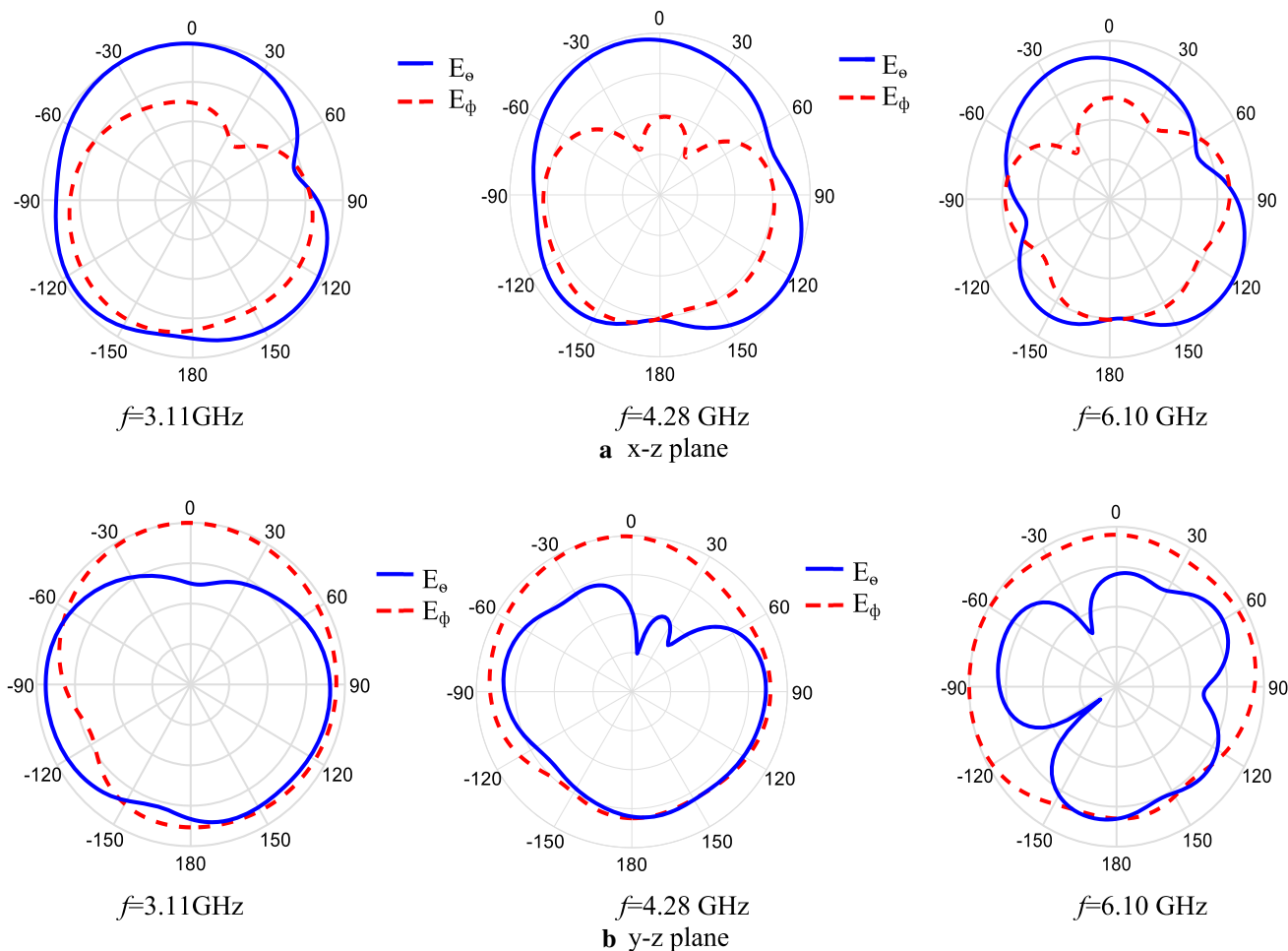


Fig. 13 The radiation fields for UWB antenna in different planes

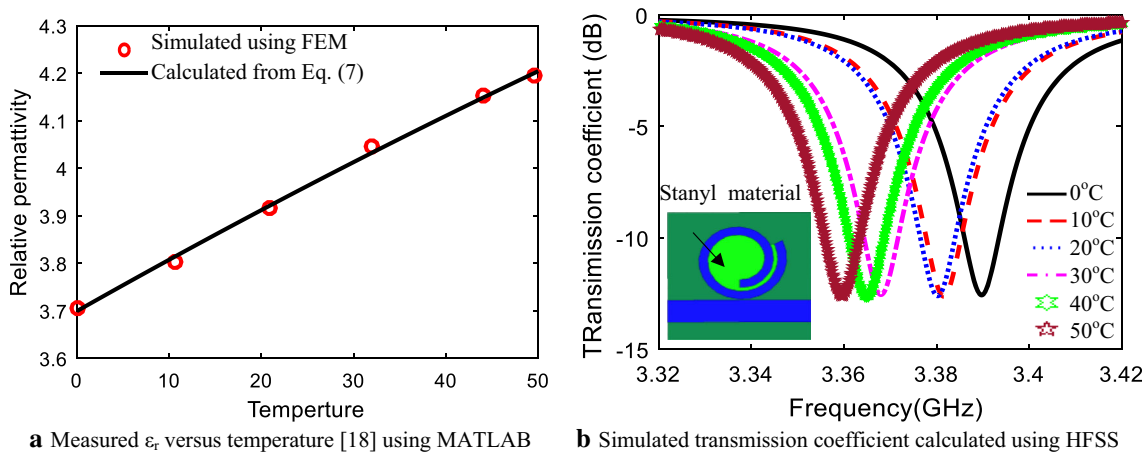


Fig. 14 The response of single bit tag integrated with Stanyl material at different temperatures

constant 3.55, loss tangent 0.0027 and thickness 0.88 mm and is fed using microstrip line (http://www.abgrp.co.uk/downloads/abgdatasheets/Nylon_4.6-Stanyl-.pdf). The microstrip width W is 3.5 mm and rectangular patch parameters ($L_l = 16.5$ mm, $W_l = 12$ mm, $L_g = 10$ mm,

$W_g = 30$ mm the feed gap $g = 1.5$ mm), substrate size $L \times W_g = 33 \times 30$ mm². The UWB monopole antenna layout with microstrip feed and parameters are presented in Fig. 12a. The rectangular monopole antenna is etched on the top side of the substrate. A partial ground plane is

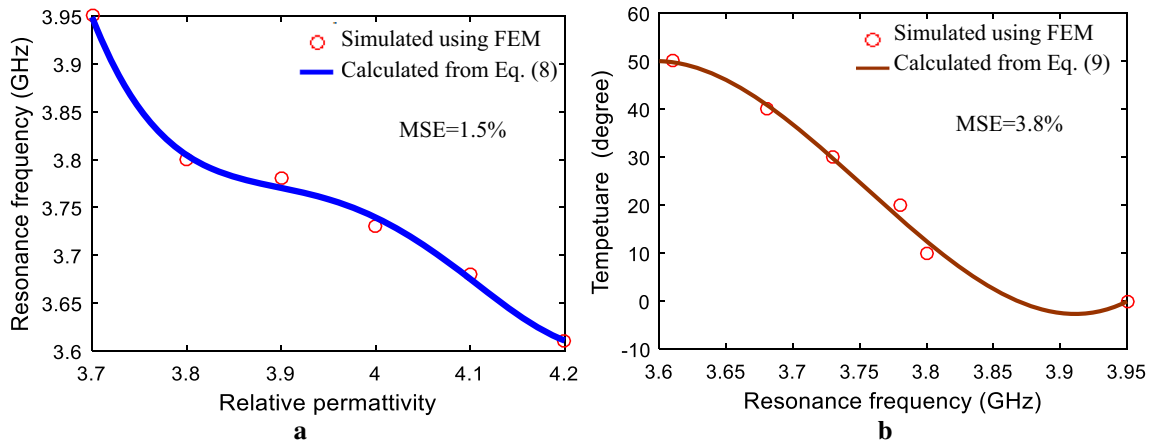


Fig. 15 Simulated resonant frequency versus a. ϵ_r , and b. T for the Stanyl polyamide material using MATLAB

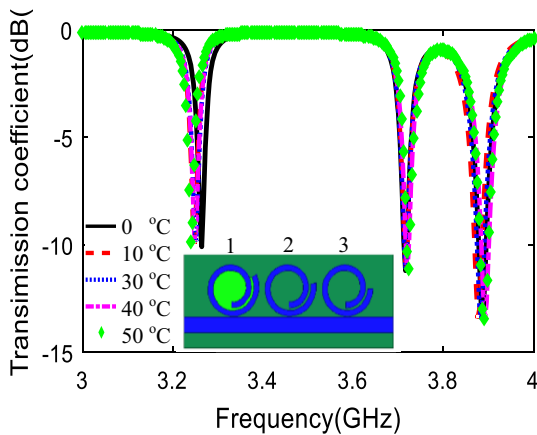


Fig. 16 The transmission coefficient of 3-bits chipless tag with ID of 000 integrated with Stanyl material calculated using HFSS

etched on the bottom side of the substrate. The feed line is a 50Ω microstrip line of width W_f . The total size of the antenna is $33 \times 30 \times 0.88 \text{ mm}^3$. The layout parameters of the antenna and its performance are shown in Fig. 12b. The radiation patterns in different planes at 3.11 GHz,

4.28 GHz and 6.10 GHz are plotted in Fig. 13. The same radiation distribution is achieved at different frequencies.

4 Chipless RFID temperature sensor

In chipless RFID tag, the temperature sensor is used by implementing the change in temperature either to the tag antenna or to the ID code generation circuit. The chipless RFID tag is proposed to have dual performance of tagging and sensing temperature. This tag structure integrates the tag antenna with temperature sensor. The surface of the curl is covered by material with electrical properties change with temperature. The resonant frequency of a single curl depends on the temperature. However, the other resonators retain their frequency response. Thus the first $N - 1$ curls of a N bit tag can be used for data encoding whereas the N th curl resembles the temperature variation of the environment. Stanyl material stands with high loads and stresses at high temperatures and exposure to aggressive environments with thermal expansion coefficient of

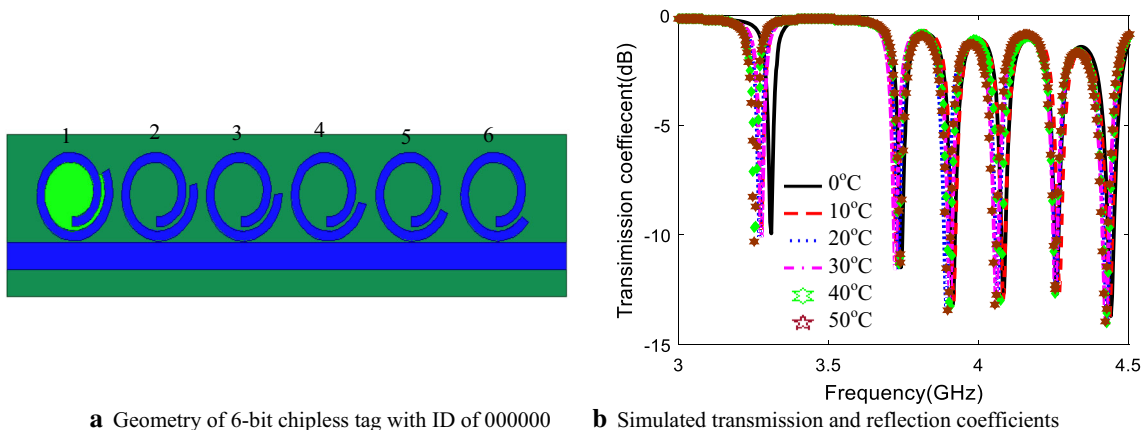


Fig. 17 The frequency response of 6-bit chipless tag with ID of 000000 integrated with Stanyl material calculated using HFSS

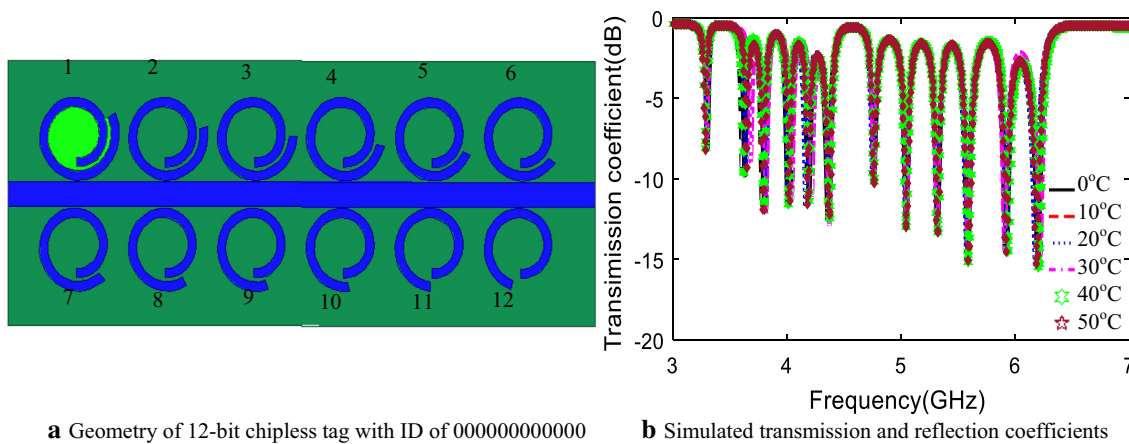
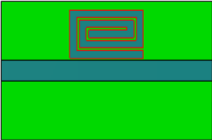
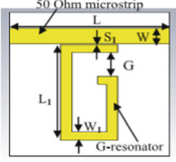
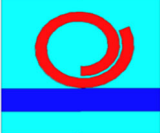


Fig. 18 The frequency response of 12-bit chipless tag with ID of 000000000000 integrated with Stanyl material calculated using HFSS

Table 3 Comparison between different chipless RFID tags

No	Types of chipless RFID resonator	Shapes	Attenuation	Size
Preradovic et al. (2009)	Spiral Resonator Chipless Tag		Resonance at 2.37 GHz with 7 dB attenuation and $S_{11} = -5.2$ dB	The dimensions of 6-bits of the code are 128.17 mm × 60 mm
Abdulkawi et al. (2018)	G-shape Resonator Chipless Tag		Resonance at 3.85 GHz with 18 dB attenuation	The dimensions of 10-bits of the code are 60 mm × 30 mm
	Proposed		Resonance at 3.12 GHz with 10 dB attenuation and $S_{11} = -3.2$ dB	The dimensions of 12-bits of the code are 49.5 mm × 34 mm

(0.2×10^{-4} ppm/°C) (Amin and Karmakar 2011). It is characterized by a linear variation of dielectric constant, ϵ_r , with temperature, T as shown in Fig. 14a. The curve is fitted using MATLAB with mean square error (MSE) of 0.22% by:

$$\epsilon_r = 1.7 \times 10^{-5}T^2 + 0.01T + 3.6 \tag{7}$$

The proposed tag structure is integrated with temperature sensing material in a single bit, where the resonant frequency depends on the temperature. However, the other resonators retain their frequency response. Figure 14b shows the single element of curl resonator covered by Stanyl TE200F6 polyamide. The variations of transmission coefficient magnitude versus frequency for temperature variation from 0 to 50 °C are shown in Fig. 14b. Increasing

temperature reduces the resonant frequency with nearly the same attenuation and bandwidth.

When the temperature, T, is changed the permittivity, ϵ_r , of the Stanyl material and hence shifts the resonant frequency down. The relationships between resonant frequency variation with T and ϵ_r are plotted in Fig. 15 and are modelled using MATLAB the equations:

$$f_o = 29.1\epsilon_r^4 - 446.9\epsilon_r^3 - 2801\epsilon_r^2 - 7464\epsilon_r + 7458 \tag{8}$$

$$T = 3406f_o^3 - 38361f_o^2 + 1.45 \times 10^5 f_o + 1.7 \times 10^5 \tag{9}$$

Good agreement between the simulated data and the fitted equation with MSE of 1.5% and 3.8%. The curl having lowest resonant frequency is modified with Stanyl polyamide in the simulation layout. The geometry of 3 bits chipless RFID tag with Stanyl polyamide material

integrated in first curl resonator. The resonant frequency of the first bit (LSB) is used for temperature sensing while the other bits include the data as plotted in Fig. 16. Figures 17 and 18 shows the 6-bits with ID 000000 and 12-bits with ID 000000000000 chipless tags integrated with Stanyl material in the LSE respectively. The variation of temperature affects only the lowest resonant frequency while the other resonant frequencies remain constant. Hence, the shift of resonant frequency of a single curl emulates the temperature variation and the other curls represents the encode data bits. A Comparison between different Chipless RFID tags is listed in Table 3.

5 Conclusion

This paper investigates a curl shape resonator for RFID chipless tag. The multi-resonator curl is used for encoding data by changing its length. It operates in 3–7 GHz band with single and multi-bit tag. The transmission coefficient, magnitude and phase, is used to indicate the coded signal. Integration of circular UWB microstrip monopoles and curl resonators to form a chipless tag are presented. The encoding of data is performed by inserting a cut in order to shift the curl resonant frequency outside the band of interest. Temperature sensor chipless RFID tag is proposed having dual performance of tagging and sensing temperature simultaneously. Two simulation programs CST-MWS and HFSS are used to analyze and calculate the RFID tag properties and MATLAB is used to mathematical modelling of this response.

Author contribution All the authors contribute equally in this paper.

Funding Open access funding provided by The Science, Technology & Innovation Funding Authority (STDF) in cooperation with The Egyptian Knowledge Bank (EKB).

Data availability The program is available upon request.

Declarations

Conflict of interest The authors have no conflicts of interest or competing interests to declare that are relevant to the content of this article. There are no supplementary materials.

Open Access This article is licensed under a Creative Commons Attribution 4.0 International License, which permits use, sharing, adaptation, distribution and reproduction in any medium or format, as long as you give appropriate credit to the original author(s) and the source, provide a link to the Creative Commons licence, and indicate if changes were made. The images or other third party material in this article are included in the article's Creative Commons licence, unless indicated otherwise in a credit line to the material. If material is not included in the article's Creative Commons licence and your intended

use is not permitted by statutory regulation or exceeds the permitted use, you will need to obtain permission directly from the copyright holder. To view a copy of this licence, visit <http://creativecommons.org/licenses/by/4.0/>.

References

- Abdulkawi WM, Sheta AFA (2018) Multi-resonator structure for small size chipless radiofrequency identification tag. *Int J Comput Digital Syst* 7(1):43–49
- Ahson S, Ilyas M (2008) RFID handbook: applications, technology, security, and privacy. Taylor & Francis Group, LLC
- Amin E and Karmakar N (2011) Development of a chipless RFID temperature sensor using cascaded spiral resonators. In: *IEEE Sensors conference*, pp 554–557, Ireland
- Chen X and Massey PJ (2006) Operating principles and features of UWB monopoles and dipoles. In: *The Institution of Engineering and Technology Seminar on Ultra Wideband Systems, Technologies and Applications 2006*, pp 131–152, Stevenage, UK
- Chung K, Kim J, Choi J (2005) Wideband microstrip-fed monopole antenna having frequency band notch function. *IEEE Microwave Wirel Compon Lett* 15(11):766–768
- Das R (2006) Chipless RFID—the end game. ID TechEx internet article. <http://www.idtechex.com/products/en/articles/00000435.asp>. (Accessed: Dec 2006)
- Finkenzeller K (2003) RFID handbook, 2nd edn. John Wiley & Sons, Ltd.
- Hirvonen M (2008) Performance enhancement of small antennas and applications in RFID, Ph.D. Thesis, Helsinki University of Technology, Finland
- Jalaly I, Robertson D (2005) Capacitively-tuned split microstrip resonators for RFID barcodes. In: *2005 European Microwave Conference*, vol. 2 pp: 4, Paris, France
- Malhat HA, Zainud-Deen SH and Awadalla KH (2011) Curved dual-band dielectric resonator tag antenna for RFID applications. *Int J Radio Frequency Identific Wirel Sens Netw* 1(1):9–21
- McVay J, Hoorfar A, Engheta N (2006) Space-filling curve RFID tags. In: *IEEE Radio and Wireless Symposium*, pp 199–202, San Diego, USA
- Pawlikowski GT (2009) Effects of polymer material variations on high frequency dielectric properties. *MRS 2009 Spring Meeting*, vol. 1156, England
- Preradovic S, Karmakar NC (2010) Chipless RFID: barcode of the future. *IEEE Microwave Mag* 11:87–97
- Preradovic S, Karmakar N (2012) Multiresonator-based chipless RFID. Springer Science, London
- Preradovic S, Balbin I, Karmakar NC, Swiegers GF (2009) Multiresonator based chipless RFID system for low-cost item tracking. *IEEE Trans Microw Theory Tech* 57:1411–1419
- Vena A, Perret E, Tedjini S (2012) Design of compact and auto-compensated single-layer chipless RFID tag. *IEEE Trans Microw Theory Tech* 60(9):2913–2924
- Yazdandoost KY, Kohno R (2004) Ultra wideband antenna. *IEEE Commun Magazine* 42(6):S29–S32
- Zainud-Deen SH, Malhat HA, Awadalla KH (2009) Fractal antenna for passive UHF-RFID applications. *Progress Electromagnet Res B* 16:209–228
- Zainud-Deen SH, Malhat HA and Awadalla KH (2011a) 8×8 Near-field focused circularly polarized cylindrical DRA array for RFID applications. *Elect Electron Eng J1*(1):9–21
- Zainud-Deen SH, Malhat HA and Awadalla KH (2011b) Octafilar helical antenna for handheld UHF-RFID reader. *Int J Radio Frequency Identific Wirel Sens Netw* 1(1):42–48

Zainud-Deen SH, Gaber SM, Malhat HA, Awadalla KH (2012) Multilayer dielectric resonator antenna transmitarray for near-field and far-field fixed RFID reader. *Progress Electromagnet Res C* 27:129–142

Zainud-Deen SH, Abo-elhassan MA, Malhat HA and Awadalla KH (2013) Simple microstrip bandstop resonators for chipless RFID

tag. In: National Radio Science Conference, (NRSC 2013), B9, pp 73–81, Cairo, Egypt

Publisher's Note Springer Nature remains neutral with regard to jurisdictional claims in published maps and institutional affiliations.